Physics and Imaging in Radiation Oncology 33 (2025) 100709

Contents lists available at ScienceDirect

Physics and Imaging in Radiation Oncology

journal homepage: www.sciencedirect.com/journal/physics-and-imaging-in-radiation-oncology

Micro silica bead scintillators for the relative dosimetry of a stereotactic radiosurgery unit

Chris J. Stepanek [a], Jack D. Aylward [a,b], Ronald Hartley-Davies [a], Lucy Winch [a,*]

[a] Department of Medical Physics and Bioengineering, Bristol Haematology & Oncology Centre, University Hospitals Bristol & Weston NHS Foundation Trust, Horfield Road, Bristol BS2 8ED, United Kingdom
[b] Medical Physics, School of Applied Sciences, University of the West of England, Bristol, United Kingdom

ARTICLE INFO

Keywords:
Micro Silica Beads
Gamma Knife relative dosimetry
Detector Output Ratios
Shot Profiles

ABSTRACT

This work describes the procedure of using Micro Silica Beads (MSBs) to verify the output factors and profiles of a stereotactic radiosurgery unit. MSBs have shown acceptable dosimetric accuracy for measurement of Detector Output Ratios (DORs) and shot profiles, down to a full width at half maximum (FWHM) of 5 mm. DORs measured with MSBs were within 1.5 % of radiochromic film, and 3 % of a microdiamond detector. Measured FWHM were within 0.2 mm of planning system and radiochromic film. MSBs can be used as an effective substitute to radiochromic film for measurement of shot profiles and DORs.

1. Introduction

Stereotactic Radiosurgery (SRS) uses finely collimated radiation fields to deliver large therapeutic doses to small benign and malignant targets, no greater than 20 cm^3 in volume, while effectively sparing the surrounding healthy tissues. These finely collimated fields present a dosimetric challenge, as only a limited subset of radiation detectors offer the spatial resolution, sensitivity and small perturbations required to accurately measure absorbed dose [1–3].

The measurement and validation of machine Output Factors (OFs) and dose profiles are essential tasks when commissioning an SRS unit. OFs quantify the absorbed dose to water ratio between a reference field and non-reference field at a specific depth. TRS-483 provides guidance on how to measure, calculate and use OFs and field output correction factors ($k^{f_{clin},f_{msr}}_{Q_{clin},Q_{msr}}$) for the quality assurance of SRS systems [4]. Due to detector perturbations and volume averaging, the ratio of detector readings acquired in output factor measurements cannot be considered equivalent to absorbed dose ratios. The term Detector Output Ratios (DORs) has been proposed to describe uncorrected estimates of field output factors [5–7]. When DORs have received field output correction, they may be considered OFs. Dose profiles, which represent the lateral spread of dose from the beam central axis, must be measured and confirmed to match those computed by the planning system. This is important as some SRS systems scale reference dose profiles with depth to calculate clinical doses.

Radiochromic film has historically been the dosimeter of choice for SRS dosimetry [7–11], however measured doses are strongly dependent on the quality of the film scanner, procedures for handling and processing films [12], and films may exhibit inhomogeneities between batches [13]. Air ionisation chamber measurements are limited by volume averaging and beam perturbation effects in small radiation fields with large dose gradients, as the presence of these detectors within the field causes lateral charged particle equilibrium to break down [6,14,15]. A range of solid state and liquid filled ion chambers with significantly smaller volumes, such as microdiamond detectors [8,9], diodes [15], liquid ionisation chambers [15] and alanine pellets [16] have proved more suitable. Groups have also reported perturbation factors for some of these detectors [15,17,18]. Several studies have reported the measurement of shot profiles using film [8,9], scanning microdiamond detectors [8,9] and plastic scintillators [9].

The use of Micro Silica Bead (MSB) scintillators in radiation dosimetry was first reported in 2014 [19]. Subsequent articles discussed their optimisation and how their application is influenced by their composition [20], mass [20], radiation response [21], processes of annealing [19,22] and readout [19,22,23]. MSBs have been shown to have good linearity over the range 1 cGy – 50 Gy [19,20], low angular dependence from 0 to 90° [19], and an energy response like soft tissue for high energy photon beams [14,20,24]. Individual MSBs have dimensions of 1.1 mm x 1.6 mm, they are predominantly composed of oxygen, silicon and sodium, have a similar density to cortical bone [14,20].

* Corresponding author.
E-mail address: lucy.winch@uhbw.nhs.uk (L. Winch).

https://doi.org/10.1016/j.phro.2025.100709
Received 15 October 2024; Received in revised form 16 January 2025; Accepted 21 January 2025
Available online 25 January 2025
2405-6316/© 2025 The Authors. Published by Elsevier B.V. on behalf of European Society of Radiotherapy & Oncology. This is an open access article under the CC BY-NC-ND license (http://creativecommons.org/licenses/by-nc-nd/4.0/).

Herein, we report a methodology for the verification of SRS OFs and shot profiles using MSBs. MSBs were used to measure DORs for the 8 mm and 4 mm shots using the 16 mm shots as the machine specific reference field. As there are currently no published field output correction factors for MSBs, MSB DORs were compared to OFs programmed into the planning system and OFs measured using established detectors. MSBs were also used to measure shot profiles which were compared with profiles calculated by the planning system and measured using film.

2. Materials and Methods

A Leksell Gamma Knife Esprit treatment unit was used with Leksell Gamma Plan (LGP) treatment planning system (version 11.3) running the TMR10 dose engine. Twenty-two MSBs (each 1.1 mm in length, 1.6 mm in width) were threaded together to form a contiguous MSB array (TrueInVivo DOSEmapper) of total length 24.2 mm (22 x 1.1 mm). Separate MSB arrays were used for each measurement and an example of an array is shown in Fig. 1. A spherical solid water phantom was used for measurements, and an insert was modified to accommodate an array by drilling a 1.8 mm diameter hole through its centre along the z-axis (schematic shown in Supplementary Fig. S1). The phantom was mounted using the GK G-Frame at a Gamma angle of 90°. An MSB array was then inserted into the phantom and a Cone Beam CT (CBCT) scan was used to ensure one of the two central beads was accurately positioned at the radiation focus (x,y,z coordinates of 100,100,100 in mm). The dose imparted to the MSBs by the CBCT scan was approximately 3000 times lower than the treatment dose and was therefore not accounted for. Once the central bead position was verified, an exposure was performed for a duration of 2.2 min. This process was performed 13 times for the 16 mm shots, 11 times for the 8 mm shots and 19 times for the 4 mm shots. After exposure, MSBs were sent to the manufacturer to be calibrated and analysed according to their published procedure [19]. Microsoft Excel was used to handle the final individual MSB data, and to calculate DORs and percentage uncertainties. DORs were calculated for each measurement by dividing the maximum dose from each 4 mm and 8 mm measurement (clinical field measurements) by the average maximum dose from the 16 mm measurements (machine specific reference field). Uncertainties were calculated by summing the standard deviation of the machine specific reference field measurements and the standard deviation of the clinical field measurements. As there are currently no field output correction factors published for MSBs, no corrections were applied. FWHM were calculated from shot profiles using the zero-crossings of an interpolating spline (scipy) fitted to a profile shifted down by half its maximum (see Supplementary Fig. S2).

EBT3 radiochromic film (Ashland Speciality Ingredients) was exposed under the same conditions as for the MSB measurements using the solid water film insert, and ten films were exposed for each collimator setting. Films were then scanned using an Epson Expression 10000XL Scanner and analysed using MyQA Patients (IBA Dosimetry, Germany) and Microsoft Excel. Z-profiles were extracted, and DORs and FWHM were calculated using the same method used for the MSBs. The batch of films were calibrated using a GK Esprit by exposing films to doses from 0 Gy to 8 Gy as calculated by planning system, and a calibration curve was produced in myQA Patients. The DORs measured using film were deemed to be equivalent to OFs due to the water equivalence of the phantom and lack of beam perturbation expected by the film.

A PTW MicroLion Type 31,080 chamber (sensitive volume = 1.7 mm^3) and a PTW microDiamond Type 60,019 (sensitive volume 0.004 mm^3) were also used to measure DORs using the solid water phantom with corresponding detector inserts. For these measurements, the charge was measured from three 60 s exposures, for each collimator size. To determine DORs, the ratio of the charge collected for each collimator relative to the average charge from the 16 mm collimator was calculated. These DORs were converted to OFs by multiplying the DORs by

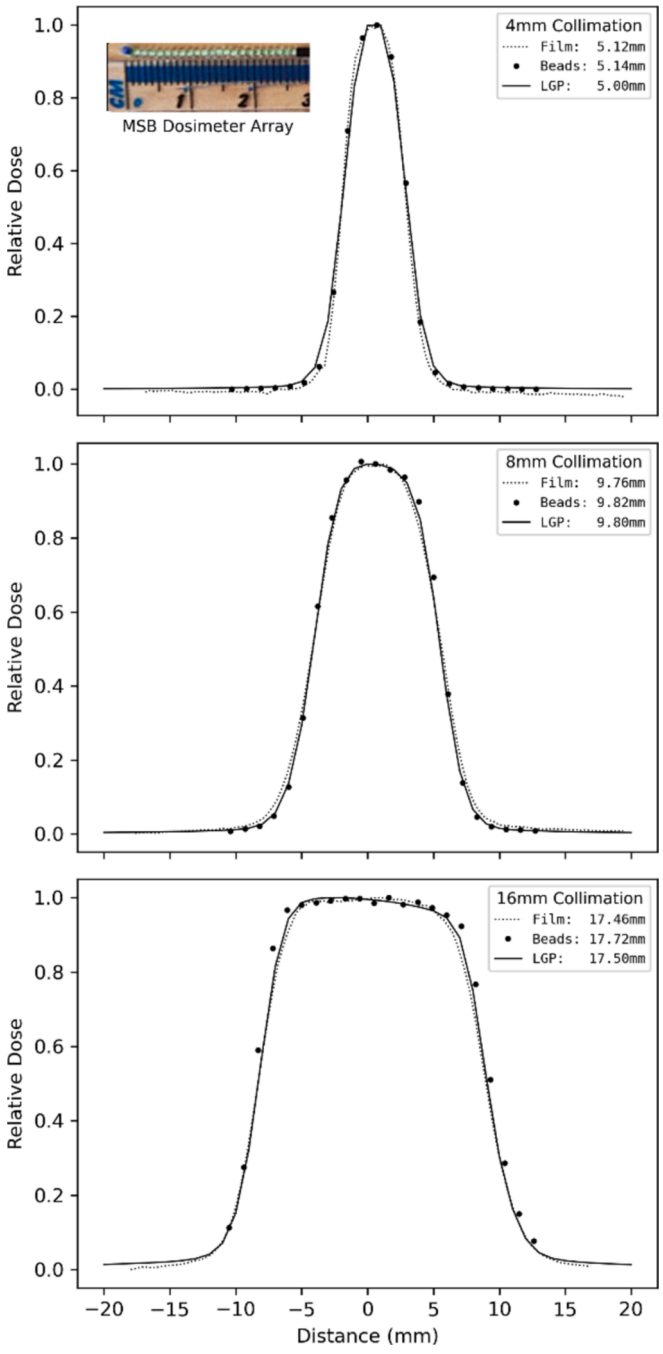

Fig. 1. Z-axis profiles of 16 mm, 8 mm and 4 mm shots measured using an MSBs and radiochromic film compared with the planning system. Average FWHM also shown. Inset, an example photo of an MSB array.

$k^{f_{clin},f_{msr}}_{Q_{clin},Q_{msr}}$ reported in [4] for the microDiamond detector and [15] for the MicroLion.

Reference dose profiles were obtained from the planning system using exported DICOM RT-Dose objects (1 x 1 x 1 mm spatial resolution).

3. Results

3.1. DORs/OFs

Table 1 shows all measured DORs and OFs and results from published literature. Average DORs measured using MSBs for 8 mm and 4 mm collimations were 0.896 and 0.795, respectively, which represent

Table 1
DORs, OFs and Z-axis profile FWHM from our work and published literature [1,8–10]. Percentage differences between measurements and data from the treatment planning system also shown. Standard deviation for 16 mm DOR/OF measurements also shown.

Dosimetry System	DORs			FWHM		
	16 mm	8 mm	4 mm	16 mm	8 mm	4 mm
MSBs	Taken as unity. (±1.6 %)	0.880 (−2.3 %) 0.866 (−3.9 %) 0.937 (3.9 %) 0.893 (−0.9 %) 0.898 (−0.3 %) 0.927 (2.9 %) 0.873 (−3.2 %) 0.906 (0.5 %) 0.886 (−1.7 %) 0.896 (−0.5 %) 0.888 (−1.4 %)	0.791 (−2.9 %) 0.799 (−1.8 %) 0.787 (−3.4 %) 0.768 (−5.8 %) 0.821 (0.9 %) 0.776 (−4.8 %) 0.789 (−3.1 %) 0.767 (−6.0 %) 0.803 (−1.4 %) 0.799 (−1.8 %) 0.796 (−2.3 %) 0.786 (−3.6 %) 0.803 (−1.3 %) 0.795 (−2.4 %) 0.846 (3.8 %) 0.788 (−3.3 %) 0.815 (0.2 %) 0.794 (−2.5 %) 0.785 (−3.6 %)	17.5 17.9 17.7 17.8 18.0 17.7 17.8 17.2 17.8 17.4 18.0 18.2 17.5	10.3 10.1 10.0 9.5 10.0 9.8 10.0 9.6 9.8 9.6 9.6	5.3 5.0 5.1 5.3 5.1 5.4 5.3 5.2 5.1 5.0 5.1 5.2 5.1 5.1 5.1 5.1 5.1 5.1
Dosimetry System	**OFs**			**FWHM**		
	16 mm	**8 mm**	**4 mm**	**16 mm**	**8 mm**	**4 mm**
Treatment Planning System	Taken as unity.	0.901	0.814	17.5	9.8	5.0
Micro Diamond Detector	Taken as unity. (±0.0 %)	0.892 (−1.0 %) [a]0.893 (−0.9 %) [a]0.895 (−0.7 %) [a]	0.819 (+0.6 %) [a]0.813 (−0.1 %) [a]0.821 (+0.9 %) [a]			
Radiochromic film	Taken as unity. (±1.6 %)	0.866 (−4.0 %) 0.914 (+1.4 %) 0.911 (+1.1 %) 0.879 (−2.5 %) 0.893 (−0.9 %) 0.898 (−0.4 %) 0.930 (+3.2 %) 0.910 (+1.0 %)	0.787 (−3.4 %) 0.825 (+1.3 %) 0.787 (−3.4 %) 0.830 (+1.9 %) 0.845 (+3.8 %) 0.799 (−1.9 %) 0.801 (−1.6 %) 0.784 (−3.7 %)	17.6 17.4 17.5 17.4 17.5	9.8 9.7 9.8 9.8 9.9	5.2 5.1 5.2 5.1 5.1

Table 1 (*continued*)

Dosimetry System	DORs			FWHM		
	16 mm	8 mm	4 mm	16 mm	8 mm	4 mm
		0.914 (+1.4 %) 0.886 (−1.7 %)	0.804 (−1.2 %) 0.805 (−1.1 %)			
Micro Lion Chamber	Taken as unity.	0.888 (−1.4 %) [b]	0.830 (+1.9 %) [b]			
Radiochromic Film from literature	Taken as unity.	0.926 (+2.8 %) [8] 0.887 (−1.5 %) [1] 0.908 (+0.8 %) [10]	0.83 (+2.0 %) [8] 0.797 (−2.1 %) [1] 0.809 (−0.6 %) [10]	17.4 [9] 17.3 [8]	9.8 [9] 9.7 [8]	5.0 [9] 4.9 [8]
Micro Diamond Detector from literature	Taken as unity.	0.897 (−0.3 %) [8] 0.902 (+0.1 %) [10]	0.829 (+1.8 %) [8] 0.827 (+1.6 %) [10]	17.4 [9] 17.4 [8]	9.8 [9] 9.7 [8]	5.0 [9] 4.9 [8]
W2 Scintillator from literature				17.5 [9]	9.8 [9]	5.1 [9]

[a] Corrected using field output correction ($k^{f_{clin},f_{msr}}_{Q_{clin},Q_{msr}}$) from [4].

[b] Corrected using field output correction ($k^{f_{clin},f_{msr}}_{Q_{clin},Q_{msr}}$ from [15].

differences of −0.6 % and −2.3 % compared with the planning system. The microdiamond detector measured average OFs of 0.893 (−0.8 %) and 0.818 (+0.5 %) for 8 mm and 4 mm, respectively, and film measured average OFs of 0.900 (−0.1 %) and 0.807 (−0.9 %), respectively. The MicroLion chamber measured OFs of 0.888 (−1.4 %) and 0.830 (+1.9 %), for 8 mm and 4 mm shots, respectively.

3.2. Uncertainties

Overall uncertainties of the 8 mm and 4 mm MSB DORS were 3.9 % and 3.9 %, respectively. These were similar to those obtained for the film measurements (3.6 % and 4.0 %, respectively). Uncertainties were smallest for measurements using the microdiamond detector (0.2 % and 0.5 %, for 8 mm and 4 mm shots, respectively), and not enough measurements were acquired with the MicroLion detector to have confidence of uncertainty.

3.3. Shot profiles

Fig. 1 shows shot profiles measured using the MSBs, film and calculated by the planning system. Table 1 shows all FWHM and results from published literature. FWHM calculated for 16 mm, 8 mm and 4 mm shot profiles measured by MSBs were 17.7 ± 0.3 mm, 9.8 ± 0.2 mm, and 5.1 ± 0.1 mm, respectively. These values represent differences from the reference by + 0.2 mm, 0.0 mm and + 0.1 mm, respectively. FWHM calculated for 16 mm, 8 mm and 4 mm film profiles were 17.5 ± 0.1 mm, 9.8 ± 0.1 mm and 5.1 ± 0.0 mm, respectively, which represent differences of −0.1 mm, 0.0 mm, and 0.1 mm.

4. Discussion

This work describes the procedure of using MSBs to verify that OFs and shot dose profiles calculated by the planning system and produced by the radiation unit are consistent. The microdiamond detector

provided OFs that were most like the planning system (<1% difference for all shots) and demonstrated the smallest uncertainties. The 8 mm DORs measured using MSBs were within 1 % of the planning system, microdiamond, Micro Lion and film measurements. The 4 mm DORs measured by MSBs were within 1.5 % of film and within 3 % of the planning system and microdiamond. The MicroLion measurements were almost 2 % greater than the planning system. While the film and microdiamond measurements in this work were all within 1 % of the planning system, other groups have reported differences between 1.6 – 2.8 % between planning system OFs and OFs measured using microdiamond and film [1,8,10]. For the latter in particular, radiotherapy departments will have their own protocols for the handling and analysis of films which may contribute significant variation. Conversely, a benefit of the MSBs is that the analysis procedure [19] is standardised, which may provide more meaningful comparison of published MSB measurements.

The MSBs and film demonstrated uncertainties of 3–4 % for 8 mm and 4 mm shots, although uncertainties using film > 4 % have been reported elsewhere [10]. The standard deviation of the 16 mm measurements using MSBs was 1.6 % which is consistent with the 1.7 % uncertainty reported in [19] for the whole measurement and readout process. The standard deviations of the 8 mm and 4 mm DORs were 2.3 % and 2.3 %, respectively. Therefore, measurement of the smaller shots contributed 0.7 % additional uncertainty.

The MSBs also provided profile measurements with FWHM that were within 0.3 mm of the planning system and were at most 0.3 mm different from literature reports that used microdiamond detectors, W2 scintillators and film [8,9]. Overall, the MSBs provided satisfactory measurements of DORs and shot profiles and could serve as a lower-cost, less laborious dosemeter with acceptable uncertainties.

There are however some requirements and limitations of using MSBs for SRS dosimetry. A solid water phantom insert needed to be modified with a 1.8 mm diameter channel, to accurately fit the MSB array. The MSBs also required accurate positioning which was achieved using the GK onboard CBCT system to position one of the two central beads at the radiation focus. While measurement of the 16 mm and 8 mm shots did not require as careful positioning of the beads, in the case of the 4 mm shots, it was essential to position a central bead at the radiation focus. Based on the increased uncertainty of measuring doses from the smallest collimator settings, we would recommend at least three measurement repeats for the 16 mm and 8 mm shots and at least five measurement repeats for the 4 mm shots. Only z-axis measurements were performed in this work as the design of the solid water phantom only permits z-axis measurements. The FWHMs reported in this work were estimated from a small number of points, therefore, these values may be sensitive to the interpolation method used.

Declaration of competing interest

The authors declare the following financial interests/personal relationships which may be considered as potential competing interests: The authors would like to acknowledge the support given by TrueInVivo® Ltd who provided technical support when required. TrueInVivo® Ltd did not however, provide any arbitration of our work.

Acknowledgements

We would like to thank Katherine Addison of the Bristol Haematology & Oncology Centre Radiotherapy Physics Unit for her assistance in proofreading this article.

Appendix A. Supplementary data

Supplementary data to this article can be found online at https://doi.org/10.1016/j.phro.2025.100709.

References

[1] Zeverino M, Jaccard M, Patin D, Ryckx N, Marguet M, Tuleasca C, et al. Commissioning of the Leksell Gamma Knife ® Icon ™. Med Phys 2017;44:355–62. https://doi.org/10.1002/mp.12052.
[2] P. Francescon P, Beddar S, Satariano N, Das IJ. Variation of k for the small-field dosimetric parameters percentage depth dose, tissue-maximum ratio and off-axis ratio. Med Phys. 2014; 41:101708 - https://doi.org/10.1118/1.4895978.
[3] Hartmann GH, Zink K. Decomposition of the dose conversion factor based on fluence spectra of secondary charged particles: Application to lateral dose profiles in photon fields. Med Phys 2018;45:4246. https://doi.org/10.1002/mp.13081.
[4] Dosimetry of small static fields used in external beam radiotherapy: an IAEA-AAPM International Code of Practice for reference and relative dose determination. Technical reports series no. 483. Vienna: International Atomic Energy Agency, 2017.
[5] Alfonso R, Andreo P, Capote M, Saiful Huq M, Kilby W, Kjäll P, et al. A new formalism for reference dosimetry of small and nonstandard fields. Med Phys 2008; 35:5179–86. https://doi.org/10.1118/1.3005481.
[6] Palmans H, Andreo PM, Huq MS, Suentjens J, Christaki KE, Meghzifene A. Dosimetry of small static fields used in external photon beam radiotherapy: Summary of TRS-483, the IAEA–AAPM international Code of Practice for reference and relative dose determination. Med Phys 2018;45:e1123–45. https://doi.org/10.1002/mp.13208.
[7] Kim TH, Yang HJ, Jeong JY, Schaarschmidt T, Kim YK, Chung HT. Feasibility of isodose-shaped scintillation detectors for the measurement of gamma knife output factors. Med Phys 2022;49:1944–54. https://doi.org/10.1002/mp.15469.
[8] Maraghechi B, Kim T, Mitchell TJ, Goddu SM, Dise J, Kavanaugh JA, et al. Filmless quality assurance of a Leksell Gamma Knife® Icon™. J Appl Clin Med Phys 2021; 22:59–67. https://doi.org/10.1002/acm2.13070.
[9] Rudek B, Bernstein OS, Qu T. Replacing gamma knife beam-profiles on film with point-detector scans. J Appl Clin Med Phys 2022;23:e13522. https://doi.org/10.1002/acm2.13522.
[10] Mancosu P, Reggiori G, Stravato A, Gaudino A, Lobefalo F, Palumbo V, et al. Evaluation of a synthetic single crystal diamond detector for relative dosimetry on the Leksell Gamma Knife Perfexion radiosurgery system. Med Phys 2015;42: 5035–41. https://doi.org/10.1118/1.4927569.
[11] Novotny J, Bhatnagar JP, Quader MA, Bednarz G, Lunsford LD, Huq MS. Measurement of relative output factors for the 8 and 4 mm collimators of Leksell Gamma Knife Perfexion by film dosimetry. Med Phys 2009;36:1768–74. https://doi.org/10.1118/1.3113904.
[12] Soares CG. Radiochromic film dosimetry. Radiat Meas 2006;41:S100–16. https://doi.org/10.1016/j.radmeas.2007.01.007.
[13] Darafsheh A. Radiation Therapy Dosimetry: A Practical Handbook. 1st ed. CRC Press; 2021. https://doi.org/10.1201/9781351005388.
[14] Jafari SM, Jordan TJ, Hussein M, Bradley DA, Clark CH, Nisbet A, et al. Energy response of glass bead TLDs irradiated with radiation therapy beams. Rad Phys Chem 2014;104:208–11. https://doi.org/10.1016/j.radphyschem.2014.03.009.
[15] Benmakhlouf H, Johansson J, Paddick I, Andreo P. Monte carlo calculated and experimentally determined output correction factors for small field detectors in Leksell Gamma Knife Perfexion beams. Phys Med Biol 2015;60:3959. https://doi.org/10.1088/0031-9155/60/10/3959.
[16] Mack A, Scheib SG, Major J, Gianolini S, Pazmandi G, Fiest H, et al. Precision dosimetry for narrow photon beams used in radiosurgery – Determination of Gamma Knife ® output factors. Med Phys 2002;29:2080–9. https://doi.org/10.1118/1.1501138.
[17] Zoros E, Moutsatsos A, Pappas EP, Georgiou E, Kollias G, Karaiskos P, et al. Monte Carlo and experimental determination of correction factors for gamma knife perfexion small field dosimetry measurements. Phys Med Biol 2017;62:7532. https://doi.org/10.1088/1361-6560/aa8590.
[18] Veselsky T, Novotny Jr J, Pastykova V, Koniarova I. Determination of small field synthetic single-crystal diamond detector correction factors for Cyberknife, Leksell Gamma Knife Perfexion and linear accelerator. Phys Med 2017;44:67–71. https://doi.org/10.1016/j.ejmp.2017.11.010.
[19] Jafari SM, Bradley DA, Gouldstone CA, Sharpe PHG, Alalawi A, Jordan TJ, et al. Low-cost commercial glass beads as dosimeters in radiotherapy. Rad Phys Chem 2014;97:95–101. https://doi.org/10.1016/j.radphyschem.2013.11.007.
[20] Jafari SM, Bates NM, Jupp T, Abdul Sani SF, Nisbet A, Bradley AD. Commercial glass beads as TLDs in radiotherapy produced by different manufacturers. Radiat Phys Chem 2017;137:181–6. https://doi.org/10.1016/j.radphyschem.2015.12.025.
[21] Jafari S. Characterisation and novel applications of glass beads as dosimeters in radiotherapy. University of Surrey); 2015. Doctoral dissertation.
[22] Ley K, Hasim SA, Lohstroh A, Shenton-Taylor C, Bradley DA. Thermoluminescent response of silica beads to high-dose irradiations. Radiat Phys Chem 2020;167: 108349. https://doi.org/10.1016/j.radphyschem.2019.108349.
[23] Knapton T, Masterson M, Parmer A, Nisbet A, Jafari S. PO-1577 Evaluation of a new automated TLD reader for silica bead radiotherapy dosimetry. Radiother Oncol 2021;161:S1302–3. https://doi.org/10.1016/S0167-8140(21)08028-2.
[24] Babaliou S, Jafari S, Palmer AL, Polak W, Sheidaei A, Shirazi A, et al. Using micro silica bead TLDs in high dose rate brachytherapy dosimetry: A phantom study.2022; 191: 109826 - https://doi.org/10.1016/j.radphyschem.2021.109826.